Bull. Chem. Soc. Jpn., 77, 2011–2020 (2004) 2011

Adsorption Equilibria of Novel Phthalocyaninatomagnesium(II) Derivatives with Thioethers at the Toluene/Water Interface

Kenta Adachi and Hitoshi Watarai*

Department of Chemistry, Graduate School of Science, Osaka University, Toyonaka, Osaka 560-0043

Received April 19, 2004; E-mail: watarai@chem.sci.osaka-u.ac.jp

Three novel phthalocyaninatomagnesium(II) derivatives with eight peripheral thioethers ($MgPc(SR)_8$) such as (2,3,9,10,16,17,23,24-octakis-ethylthiophthalocyaninato)magnesium(II) ($MgPc(SEt)_8$), (2,3,9,10,16,17,23,24-octakis-benzylthiophthalocyaninato)magnesium(II) ($MgPc(SBz)_8$), and (2,3,9,10,16,17,23,24-octakis-benzhydrylthiophthalocyaninato)magnesium(II) ($MgPc(SBh)_8$) were synthesized. The interfacial adsorption and aggregation behavior of the three derivatives in a toluene/water system were examined by means of a high-speed stirring (HSS) method and a centrifugal liquid membrane (CLM) method. The interfacial adsorption constant of each $MgPc(SR)_8$ derivative at the toluene/water interface was determined by the HSS measurement. Only in the case of $MgPc(SEt)_8$, the formation of the trimer was observed at the interface. Moreover, the CLM measurements showed that the interfacial aggregate of $MgPc(SEt)_8$ had a new broad band (613 nm) at the blue flank of the Q band (702 nm) of $MgPc(SEt)_8$ monomer, which might be ascribed to H-aggregate. Extended double-dipole (EDD) model calculations suggested a cofacially stacked arrangement of $MgPc(SEt)_8$ molecules in the trimer. The interfacial spectral change indicated that the aggregation of $MgPc(SEt)_8$ at the toluene/water interface proceeded in a two-step, three-stage (monomer → dimer → trimer) formation.

In the last quarter century, the chemistry and engineering of phthalocyanine compounds (Pc) with functional substituents have advanced remarkably, particularly in the application of these compounds in the development of fuel cells, chemical sensors, solar cells, electrophotography, and photodynamic therapy (PDT) of cancer.[1–4] For the application of Pc compounds, it is quite important to improve their solubility in common solvents. Peripheral substitution with bulky groups[5] or long alkyl chains[6] made Pc compounds more soluble in common organic solvents. The introduction of sulfonyl,[7] carboxyl,[8] or amino[9] groups gave water-soluble products. Although the structures and functions of Pcs and their metallocomplexes have been extensively studied, only a few reports have been known on Pc derivatives with eight thioether substituents in the peripheral benzene rings ($MPc(SR)_8$).[10,11] These compounds ($MPc(SR)_8$) have unique spectroscopic and photochemical properties. For example, they absorb longer wavelength light in comparison with other Pc derivatives without thioether substituents. This is a very useful feature for applications in PDT and near-IR absorbers.

Chemical reactions at interfaces between two immiscible liquids have become an important subject in various fields. Recently, the liquid/liquid interface has been recognized as an effective nano-reaction field in solvent extraction,[12] and as a model for biomembranes.[13] Therefore, it is very important to investigate the interfacial reactivity of Pc derivatives in evaluating their potential in semiconductivity, photocatalytic efficiency, and their biological significance like a porphyrin in modern interfacial nano-technology. However, studies on the reactivity of Pc at the liquid/liquid interface have rarely been performed. The poor solubility of Pc in common organic solvents might be one of the reasons.

In the present work, we synthesized three novel phthalocyaninatomagnesium(II) derivatives substituted with eight thioether groups at the peripheral benzene sites ($MgPc(SR)_8$). These derivatives showed improved solubility in common organic solvents, and the interfacial adsorption behavior of these compounds in a toluene/water system using a high-speed stirring (HSS) method[14] and a centrifugal liquid membrane (CLM) technique.[15] We report here the first example of interfacial adsorption phenomena of Pcs at the liquid/liquid interface.

1. Experimental

1.1 Material. 1-Butanol, tetrahydrofuran, chloroform, and toluene were purchased from Nacalai Tesque Inc. (Kyoto, Japan). 1-Butanol and tetrahydrofuran were freshly distilled after drying over molecular sieves before use. Chloroform was shaken three times with 2 M ($mol\,dm^{-3}$) potassium hydroxide solution, followed by shaking three times with water, dried over calcium chloride, and then fractionally distilled. Toluene was purified according to a literature method,[16] and then saturated with distilled water immediately before use. Water was distilled and deionized by a Milli-Q system (Millipore). All other chemicals were of reagent grade from Tokyo Kasei Kogyo Co., Ltd (Tokyo, Japan) or Wako Chemicals (Osaka, Japan), and were used as received without further purification.

1.2 Synthesis of Thioether-Derivatised Phthalocyaninatomagnesium(II) [$MgPc(SR)_8$]. **Diphenylmethanethiol [BhSH]:** Diphenylmethanol (30.0 g, 0.325 mol), conc. hydrochloric acid (250 mL), and thiourea (30.0 g, 0.394 mol) were mixed and refluxed for 18 h under a nitrogen atmosphere. After cooling down to room temperature, 6 M sodium hydroxide solution was added dropwise into the mixture, followed by refluxing for 3 h. After the mixture was acidified with conc. hydrochloric acid, the re-

Published on the web November 11, 2004; DOI 10.1246/bcsj.77.2011

duced oily compound was extracted into diethyl ether, and then dried over anhydrous sodium sulfate. After removal of the solvent, the residue was distilled under reduced pressure (20 Torr, 130 °C) to yield BhSH as a colorless oil. Yield of the compound: 25.0 g (76.9% on the basis of diphenylmethanol); bp 237–239 °C; ^{1}H NMR (300 MHz, CDCl$_3$) δ 2.34 (d, 1H, –S$\underline{\text{H}}$), 5.50 (d, 1H, (Ph)$_2$–C$\underline{\text{H}}$–SH), 7.29–7.50 (m, 10H, –$\underline{\text{(Ph)}_2}$); ^{13}C NMR (75 MHz, CDCl$_3$) δ 48.1, 127.5, 128.1, 128.9, 143.7.

4,5-Bis(ethylthio)phthalonitrile [Pn(SEt)$_2$]: Ethanethiol (1.86 g, 30 mmol) and 4,5-dichlorophthalonitrile (1.97 g, 10 mmol) were dissolved in absolute tetrahydrofuran 70 mL under a nitrogen atmosphere. After stirring for 30 min, finely ground anhydrous potassium carbonate (10 g, 0.43 mol) was added portionwise over 90 min with efficient stirring. The reaction mixture was stirred under a nitrogen atmosphere at around 50 °C for 12 h. Ice water (100 mL) was then added to separate any inorganic residues, and the aqueous phase was extracted with chloroform (3 times with 25 mL chloroform). The combined extracts were dried over anhydrous sodium sulfate. After the removal of the solvent, the residue was crystallized from methanol to yield Pn(SEt)$_2$ as a pale white solid. Yield of compound: 1.95 g (78.4% on the basis of 4,5-dichlorophthalonitrile); mp 109–111 °C; TLC $R_f = 0.60$ (chloroform); ^{1}H NMR (300 MHz, CDCl$_3$) δ 1.37 (t, 6H, S–C–$\underline{\text{CH}_3}$), 2.97–3.00 (m, 4H, S–$\underline{\text{CH}_2}$–C), 7.36 (s, 2H, S–$\underline{\text{Ar}}$–CN); ^{13}C NMR (75 MHz, CDCl$_3$) δ 13.4, 27.0, 111.4, 115.8, 128.4, 144.2; FT-IR (KBr, cm^{-1}) 2974, 2932, 2227 (C≡N), 1562, 1461, 1431, 1377, 1345, 1229 (C–S–C), 1117, 1050, 961, 928, 895, 528; Anal. Calcd for $C_{12}H_{12}N_2S_2$: C, 58.03; H, 4.87; N, 11.28%. Found: C, 57.97; H, 4.77; N, 11.52%.

4,5-Bis(benzylthio)phthalonitrile [Pn(SBz)$_2$]: Using a similar procedure to that of Pn(SEt)$_2$, the reaction of benzylthiol (3.72 g, 30 mmol) with 4,5-dichlorophthalonitrile (1.97 g, 10 mmol) gave Pn(SBz)$_2$ as a pale white solid. Yield of compound: 3.01 g (80.9% on the basis of 4,5-dichlorophthalonitrile); mp 173–174 °C; TLC $R_f = 0.77$ (chloroform); ^{1}H NMR (300 MHz, CDCl$_3$) δ 4.22 (s, 2H, Ph–$\underline{\text{CH}_2}$–S), 7.28–7.36 (m, 10H, –$\underline{\text{Ph}}$), 7.42 (s, 2H, S–$\underline{\text{Ar}}$–CN); ^{13}C NMR (75 MHz, CDCl$_3$) δ 36.9, 111.8, 114.6, 128.6, 129.0, 129.4, 133.5, 136.4; FT-IR (KBr, cm^{-1}) 2919, 2851, 2227 (C≡N), 1564, 1494, 1461, 1346, 1237 (C–S–C), 1115, 1070, 1029, 962, 889, 873, 711, 694, 529; Anal. Calcd for $C_{22}H_{16}N_2S_2$: C, 70.93; H, 4.33; N, 7.52%. Found: C, 70.60; H, 4.23; N, 7.58%.

4,5-Bis(benzhydrylthio)phthalonitrile [Pn(SBh)$_2$]: Similar to Pn(SEt)$_2$, the reaction of diphenylmethanethiol (3.00 g, 15 mmol) with 4,5-dichlorophthalonitrile (0.98 g, 5 mmol) afforded Pn(SBh)$_2$ as a pale white solid. Yield of compound: 2.23 g (85.1% on the basis of 4,5-dichlorophthalonitrile); mp 143–145 °C; TLC $R_f = 0.79$ (chloroform); ^{1}H NMR (300 MHz, CDCl$_3$) δ 5.72 (s, 2H, (Ph)$_2$–$\underline{\text{CH}}$–S), 7.23–7.37 (m, 20H, –$\underline{\text{Ph}}$), 7.43 (s, 2H, S–$\underline{\text{Ar}}$–CN); ^{13}C NMR (75 MHz, CDCl$_3$) δ 56.4, 112.0, 115.3, 128.5, 128.7, 131.3, 138.7, 138.7, 143.8; FT-IR (KBr, cm^{-1}) 2970, 2922, 2231 (C≡N), 1566, 1493, 1450, 1341, 1226 (C–S–C), 1110, 1077, 1030, 928, 898, 872, 746, 699, 623; Anal. Calcd for $C_{34}H_{24}N_2S_2$: C, 77.83; H, 4.61; N, 5.34%. Found: C, 77.73; H, 4.58; N, 5.00%.

(2,3,9,10,16,17,23,24-Octakis-ethylthiophthalocyaninato)-magnesium(II) [MgPc(SEt)$_8$]: In following the procedure of a classic Linstead macrocyclization.[17] Metal magnesium (0.67 g, 12.8 mmol) was dissolved in refluxing 1-butanol (10 mL) during 12 h with the aid of an iodine crystal (ca. 0.1 g) as initiator. To the resulting magnesium butoxide suspension was added Pn(SEt)$_2$ (0.7 g, 2.8 mmol) as a slurry in 5 mL of 1-butanol. The combined mixture was refluxed for 6 h under a nitrogen atmosphere. The solvent was removed under reduced pressure, and the resulting dark green solid was dissolved in chloroform (25 mL). The resulting solution was washed with 25 mL of water four times, dried over absolute magnesium sulfate, and evaporated in vacuum. The reduced was treated in a Soxhlet apparatus with acetone until the solvent turned colorless, and then dried in vacuum. The crude product was further subjected to silica column chromatography eluted with a chloroform–methanol (9:1 v/v) mixed solvent, and pure MgPc(SEt)$_8$ was yielded as a dark green solid. This compound was soluble in chloroform, dichloromethane, toluene, DMSO, and DMF. Yield of compound: 0.353 g (49.6% on the basis of Pn(SEt)$_2$); mp > 250 °C; TLC $R_f = 0.91$ (chloroform: methanol = 9:1); ^{1}H NMR (300 MHz, DMSO-d_6) δ 1.70 (t, 24H, S–C–$\underline{\text{CH}_3}$), 3.51 (d, 16H, S–$\underline{\text{CH}_2}$–C), 8.74 (s, 8H, Ar); FT-IR (KBr, cm^{-1}) 2968, 2925, 2868, 1592, 1476, 1446, 1403, 1369, 1331, 1262 (C–S–C), 1181, 1066, 943, 777, 747; MALDI-TOF/MS m/z 1018 ($M + H^+$) [matrix: α-cyano-4-hydroxycinnamic acid (α-CHCA)]; Anal. Calcd for $C_{48}H_{48}MgN_8S_8$: C, 56.64; H, 4.75; N, 11.01%. Found: C, 56.81; H, 4.74; N, 10.57%.

(2,3,9,10,16,17,23,24-Octakis-benzylthiophthalocyaninato)-magnesium(II) [MgPc(SBz)$_8$]: In a similar manner to that of MgPc(SEt)$_8$, the cyclotetramerization reaction of Pn(SBz)$_2$ (1.00 g, 2.68 mmol) yielded MgPc(SBz)$_8$ as a dark green solid. This product was soluble in chloroform, dichloromethane, toluene, DMSO, and DMF. Yield of compound: 0.586 g (57.8% on the basis of Pn(SBz)$_2$); mp > 250 °C; TLC $R_f = 0.88$ (chloroform: methanol = 9:1); ^{1}H NMR (300 MHz, DMSO-d_6) δ 4.78 (s, 16H, S–$\underline{\text{CH}_2}$–Ph), 7.29 (t, 8H, –Ph$_{(1)}$), 7.39 (t, 16H, –Ph$_{(2)}$), 7.70 (d, 16H, –Ph$_{(3)}$); FT-IR (KBr, cm^{-1}) 2922, 2851, 1590, 1494, 1451, 1402, 1368, 1283 (C–S–C), 1110, 1066, 943, 774, 747, 699; MALDI-TOF/MS m/z 1513 ($M + H^+$) [matrix: α-cyano-4-hydroxycinnamic acid (α-CHCA)]; Anal. Calcd for $C_{88}H_{64}MgN_8S_8$: C, 68.80; H, 4.26; N, 7.40%. Found: C, 68.97; H, 4.22; N, 7.26%.

(2,3,9,10,16,17,23,24-Octakis-benzhydrylthiophthalocyaninato)magnesium(II) [MgPc(SBh)$_8$]: The cyclotetramerization reaction of Pn(SBh)$_2$ (1.00 g, 1.91 mmol) gave MgPc(SBh)$_8$ as a light green solid. The product was soluble in chloroform, dichloromethane, toluene, DMSO, DMF, and acetone. Yield of compound: 0.535 g (52.8% on the basis of Pn(SBh)$_2$); mp > 250 °C; TLC $R_f = 0.79$ (chloroform:methanol = 9:1); ^{1}H NMR (300 MHz, DMSO-d_6) δ 4.78 (s, 16H, S–$\underline{\text{CH}_2}$–Ph), 7.29 (t, 8H, –Ph$_{(1)}$), 7.39 (t, 16H, –Ph$_{(2)}$), 7.70 (d, 16H, –$\underline{\text{Ph}}_{(3)}$); FT-IR (KBr, cm^{-1}) 3024, 2923, 1593, 1486, 1447, 1400, 1368, 1330, 1277 (C–S–C), 1180, 1107, 1066, 942, 775, 747, 699; MALDI-TOF/MS m/z 2123 ($M + H^+$) [matrix: α-cyano-4-hydroxycinnamic acid (α-CHCA)]; Anal. Calcd for $C_{136}H_{96}MgN_8S_8$: C, 76.94; H, 4.56; N, 5.28%. Found: C, 77.35; H, 4.51; N, 5.26%.

UV–vis data of MgPc(SEt)$_8$, MgPc(SBz)$_8$, MgPc(SBh)$_8$, and unsubstituted MgPc[18] are summarized in Table 1.

1.3 High-Speed Stirring Measurement. The interfacial adsorption of MgPc(SR)$_8$ derivatives in the toluene/water system was measured by using a high-speed stirring (HSS) method. The principle of HSS method was described elsewhere,[14,19] and an analogous procedure was employed.[20–22] Fifty milliliters of the toluene phase containing MgPc(SR)$_8$ derivatives and the same volume of the aqueous phase containing 0.033 M sodium sulfate and acetate buffer (pH 6) were put into a glass stir-cell, which was thermostated by a water-jacket at 25 ± 0.1 °C. The absorption spectra of the toluene phase were measured at the stirring rate of

Table 1. UV–Vis Data of Phthalocyaninatomagnesium(II) Derivatives

Compound	$\lambda_{\max}$/nm ($\log \varepsilon$/L mol^{-1} cm^{-1})			
MgPc[a)]	674 (4.94)	644 (sh)	607 (4.12)	347 (4.36)
MgPc(SEt)$_8$	702 (5.04)	670 (sh)	632 (4.33)	368 (4.61)
MgPc(SBz)$_8$	708 (5.11)	676 (sh)	638 (4.40)	373 (4.73)
MgPc(SBh)$_8$	714 (5.39)	682 (sh)	640 (4.63)	378 (4.99)

a) In pyridine (Ref. 18), sh = shoulder.

5000 rpm and 200 rpm. The stirring rate was monitored by a speed controller (Nikko Keisoku Co. Ltd., SC-5). The toluene phase was continuously separated from the stirred two-phase system by means of a PTFE phase separator, and circulated through a flow cell installed in a photodiode-array detector (Shimadzu, SPD-M 6A) at the flow rate of 20 mL min^{-1} by a pump (Flumax Junior, Fluid Metering Inc.). Hence, we could determine the interfacial concentration of MgPc(SR)$_8$ derivatives by evaluating the difference between the absorbances of the toluene phase under high-speed stirring (5000 rpm) and low-speed stirring (200 rpm) at the absorption maximum wavelength.

The adsorption isotherms were measured from the HSS method using various concentrations of MgPc(SR)$_8$ derivatives. In the present system, Langmuir isotherm is given by[23]

$$[\mathrm{MgPc(SR)_8}]_\mathrm{i} = \frac{aK'[\mathrm{MgPc(SR)_8}]_\mathrm{o}}{a + K'[\mathrm{MgPc(SR)_8}]_\mathrm{o}}, \tag{1}$$

where $[\mathrm{MgPc(SR)_8}]_\mathrm{i}$ and $[\mathrm{MgPc(SR)_8}]_\mathrm{o}$ denote the concentration of MgPc(SR)$_8$ adsorbed at the toluene/water interface (mol/dm^2) and in the bulk toluene phase (mol/dm^3), respectively. a is the saturated interfacial concentration (mol/dm^2) and K' is the interfacial adsorption constant (dm) defined at an infinitely diluted concentration of MgPc(SR)$_8$,

$$K' = \frac{[\mathrm{MgPc(SR)_8}]_\mathrm{i}}{[\mathrm{MgPc(SR)_8}]_\mathrm{o}}. \tag{2}$$

The difference between the absorbances of the bulk toluene phase under high-speed stirring and low-speed stirring conditions, ΔA, and the absorbance of the bulk toluene phase, A_o, under the high-speed stirring can be described as follows,

$$\Delta A = \varepsilon l [\mathrm{MgPc(SR)_8}]_\mathrm{i} \frac{S_\mathrm{i}}{V_\mathrm{o}}, \tag{3}$$

$$A_\mathrm{o} = \varepsilon l [\mathrm{MgPc(SR)_8}]_\mathrm{o}, \tag{4}$$

where ε, l, S_i, and V_o are the molar absorptivity in toluene, the optical path length, the total interfacial area, and the organic phase volume, respectively. The total interfacial area in the toluene/water system was reported to be 2.0×10^2 dm^2.[24]

1.4 Centrifugal Liquid Membrane Measurement. The principles of a centrifugal liquid membrane (CLM) method were described elsewhere.[15] The apparatus for CLM method was essentially the same as the one reported previously.[25] A toluene solution (0.150 mL) of 1.0×10^{-6} M MgPc(SR)$_8$ derivatives was introduced into a cylindrical cell, whose height and outer diameter were 3.3 and 2.1 cm, respectively. When the horizontally placed cylindrical cell was rotated at around 10000 rpm, an aqueous solution (0.250 mL) containing 0.033 M sodium sulfate and acetate buffer (pH 6) was injected into the cell through a 2 mm diameter hole fabricated in the center of the flat side wall. The sum of the absorption spectra of the bulk phases and interface was measured with a UV–vis spectrophotometer (Agilent, 8453) at 1.0 s intervals with an integration time of 0.5 s. The thickness of each toluene phase and the aqueous phase was 77 μm and 128 μm, respectively. The interfacial area (S_i) between the two liquid membrane phases was calculated to be 19.4 cm^2.

1.5 Other Apparatus. Chromatographic separations were performed by a column with silica gel (Wako Gel C-200). pH Measurements were conducted using a HORIBA F-14 pH meter equipped with a HORIBA 6366-10D glass electrode. ^{1}H and ^{13}C NMR spectra were recorded on a Varian Unity 300 spectrometer. Chemical shifts of ^{1}H NMR spectra were relative to an internal standard of TMS. Infrared spectra (KBr disk) were measured using a Nicolet MAGNA-IR 560 FT-IR spectrometer. MALDI-TOF mass spectra were obtained on a PerSeptive Biosystems Voyager DE-Pro spectrometer with α-cyano-4-hydroxycinnamic acid (α-CHCA) as a matrix. Elemental analysis was done using a Perkin-Elmer series II CHNS/O analyzer 2400. UV–visible spectra were measured using a JASCO V-570 spectrometer. All melting points were taken in capillary tubes without temperature correction.

2. Results and Discussion

2.1 Synthesis of MgPc(SR)$_8$ Derivatives. Three magnesium complexes of the eight thioether substituted phthalocyanines were synthesized starting from 4,5-dichlorophthalonitrile, as shown in Scheme 1. The first step of the synthesis was to prepare a phthalonitrile with two thioethers (Pn(SR)$_8$). By nucleophilic displacement, 4,5-dichlorophthalonitrile was converted to Pn(SR)$_8$ compound with an excess of thiol in the presence of an excess amount of anhydrous potassium carbonate in tetrahydrofuran. The yield was quite high (around 80%). This synthetic procedure was previously described by Wöhrle et al.[26] and was recently improved by Ozoemena et al.[11] From Pn(SR)$_8$ compound, we could readily synthesize the corresponding MgPc(SR)$_8$ derivatives according to a cross cyclotetramerization reaction of Pn(SR)$_2$ under the classical Linstead conditions (magnesium butoxide/n-butanol).[17] A prolonged reaction time of up to 6 h resulted in a low yield for MgPc(SR)$_8$ derivatives (<20%), probably due to the decomposition of the derivatives formed. Decomposition of the peripheral thioether substituents could have occurred somewhat during the cyclotetramerization, but all results from the NMR spectra, the elemental analysis and MALDI-TOF mass spectra were in good agreement with the expected ones. Hence, we concluded that the obtained compounds were the expected ones, and had a single geometric isomer. All derivatives synthesized exhibited good solubility in common solvents (such as CHCl$_3$, DMF, DMSO, and toluene), especially in the benzhydrylthio (SBh) substituent. MgPc(SR)$_8$ derivatives were stable in these solvents, and also were stable in water or acid. No demetallation was observed by contact with water or conc. hydrochloric acid.

2.2 Dimerization of MgPc(SR)$_8$ Derivatives in Toluene. Figure 1 shows the concentration-dependence of the UV–vis absorption spectra of MgPc(SR)$_8$ derivatives. These spectra are similar to each other, as observed in unsubstituted MgPc[18] (not shown) with D_{4h} symmetry.[1] The absorption maxima of the main peaks of the Q and B bands in MgPc(SR)$_8$ derivatives appeared at around 700 and 360 nm. In the case of D_{4h} symmetry, the Q band in Pcs was attributed to the π–π^* transition from the HOMO to the LUMO of the phthalocyanine ring, and

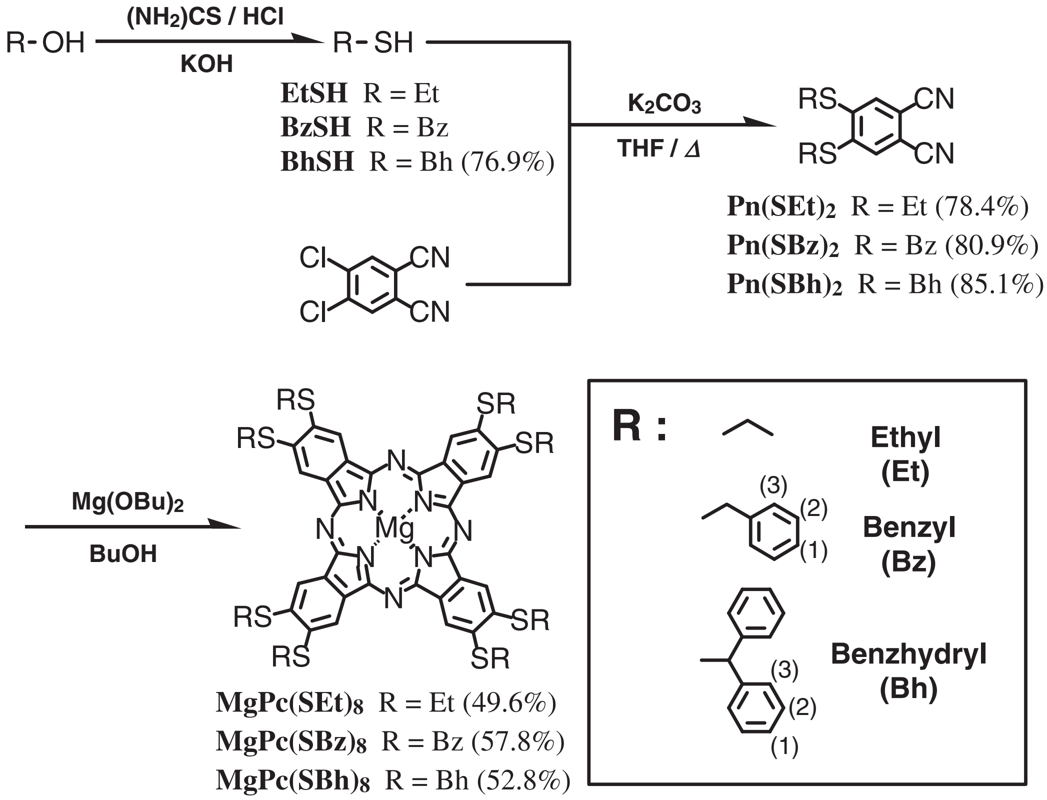

Scheme 1. Reaction routes for the syntheses of phthalocyaninatomagnesium(II) with eight peripheral thioether substituents.

the B band has been attributed to the deeper π levels–LUMO transition.[1] Both the Q and B bands in MgPc(SR)$_8$ derivatives shifted to a longer wavelength in the order MgPc(SBh)$_8$ > MgPc(SBz)$_8$ > MgPc(SEt)$_8$ > MgPc (see Table 1). Such a red shift implies that the energy gap between the HOMO and the LUMO, and that between deeper π levels and LUMO, become smaller in the same order described above.

It is noted here that the Q band of MgPc(SBh)$_8$ was unchanged over the whole concentration range (from 5.0×10^{-7} to 1.0×10^{-5} M). The Lambert–Beer relationship is shown as an inset for MgPc(SBh)$_8$ in Fig. 1c. According to this result and other reported results,[1,27,28] the branching of the benzhydryl group and its preferential solvation by toluene molecules might have prevented the aggregation of MgPc(SBh)$_8$. On the other hand, the absorption spectra of MgPc(SEt)$_8$ and MgPc(SBz)$_8$ showed a non-linear concentration dependence, e.g., the intensities of the Q bands of MgPc(SEt)$_8$ and MgPc(SBz)$_8$ gradually decreased with an increase in their concentrations, and the absorption spectra showed discernible shoulders at 655 nm (MgPc(SEt)$_8$) and 659 nm (MgPc(SBz)$_8$) in concentrations higher than 1.0×10^{-6} M. The following HSS and CLM measurements were carried out in concentrations of MgPc(SEt)$_8$ and MgPc(SBz)$_8$ in the bulk toluene less than 1.0×10^{-6} M. Isosbestic points were observed in the visible region of these spectra, indicating that the spectral changes were governed by an initial and a final species with no side reactions.[29] These concentration-dependent spectral changes are a typical feature of the dimerization known in Pc compounds.[30–33] The blue-shifting, broadening, and lowering in the intensity of the Q band clearly indicate dimerization with a "face-to-face" configuration.[30] The absorption bands of the monomer and the dimer are separated quite well, and the molar absorptivity of the monomer Q band was obtained from the absorbance in the dilute solution. The dimerization reaction is defined by,

$$2\ \text{Monomer} \overset{K_\mathrm{d}}{\rightleftharpoons} \text{Dimer} \tag{5}$$

$$\log C_\mathrm{D} = \log K_\mathrm{d} + 2 \log C_\mathrm{M} \tag{6}$$

where C_M and C_D are the concentrations of the complex in the monomer and dimer, respectively. The dimerization constants, K_d, for MgPc(SEt)$_8$ and MgPc(SBz)$_8$ in toluene were calculated from the UV–vis spectra using the approximation method of West and Pearce,[34] assuming that the observed spectrum at concentration lower than 1.0×10^{-6} M was that of the monomer. As shown in Fig. 2, the plots of $\log C_\mathrm{D}$ vs $\log C_\mathrm{M}$ for MgPc(SEt)$_8$ and MgPc(SBz)$_8$ in toluene gave straight lines, with a slope of ca. 2. The intercepts afforded the values of $\log K_\mathrm{d}$. The observed values of K_d are summarized in Table 2.

2.3 Interfacial Adsorption Behavior of MgPc(SR)$_8$ Derivatives. The interfacial adsorption of MgPc(SR)$_8$ derivatives in the toluene/water system was measured using a high-speed stirring (HSS) method. The adsorption isotherms of MgPc(SEt)$_8$, MgPc(SBz)$_8$, and MgPc(SBh)$_8$ were measured, as shown in Fig. 3. The interfacial adsorption constants, K', of MgPc(SBz)$_8$ and MgPc(SBh)$_8$ were obtained under the Nernst adsorption condition. The values of K' are also listed in Table 2. The saturated interfacial concentration, a, was not obtained, because the interfacial adsorption concentration was too low under the present total concentrations. On the oth-

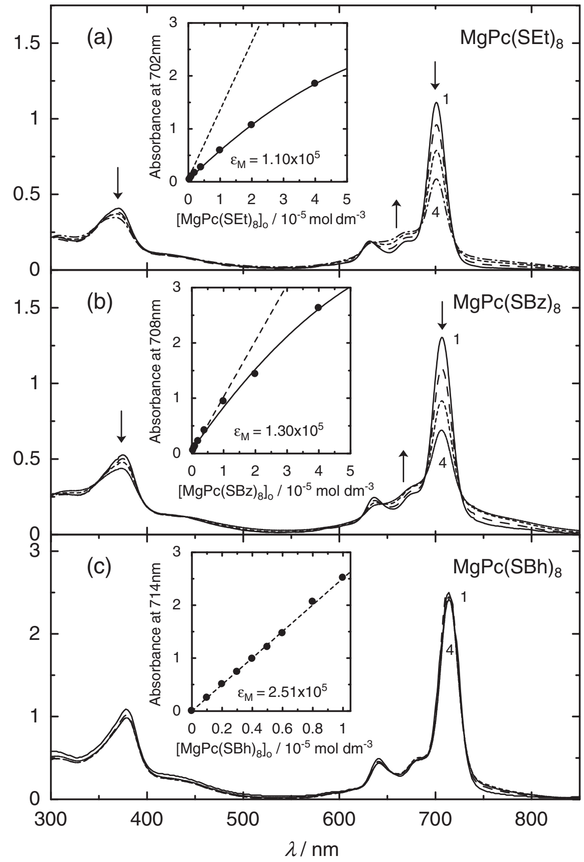

Fig. 1. Concentration dependence of absorption spectrum of MgPc(SR)_8 derivatives in toluene (top: MgPc(SEt)_8, medium: MgPc(SBz)_8, bottom: MgPc(SBh)_8): 1) 1.0×10^{-6} mol/dm^3; 2) 5.0×10^{-6} mol/dm^3; 3) 1.0×10^{-5} mol/dm^3; 4) 2.0×10^{-5} mol/dm^3. The insets show Lambert–Beer law plots for the absorbance at Q band of MgPc(SR)_8 monomer; the slopes of broken lines gave molar absorptivities of monomers, ε_M. The arrows indicate the direction of the absorbance changes with increasing concentration.

er hand, the interfacial adsorption behavior of MgPc(SEt)_8 did not obey the Langmuir isotherm. Therefore, we thought that there were two steps in the adsorption of MgPc(SEt)_8 at the toluene/water interface. The first step was the adsorption of MgPc(SEt)_8 monomer at the toluene/water interface, and the second step was the interfacial formation of the aggregate, $(\text{MgPc(SEt)}_8)_n$, from the monomer (MgPc(SEt)_8) represented by,

$$n(\text{MgPc(SEt)}_8)_\text{i} \overset{K_\text{agg}}{\rightleftharpoons} (\text{MgPc(SEt)}_8)_{n\text{i}}, \tag{7}$$

$$K_\text{agg} = \frac{[(\text{MgPc(SEt)}_8)_n]_\text{i}}{[\text{MgPc(SEt)}_8]_\text{i}{}^n}, \tag{8}$$

where K_agg and $[(\text{MgPc(SR)}_8)_n]_\text{i}$ are the aggregation constant of MgPc(SEt)_8 at the toluene/water interface and the concentration of MgPc(SR)_8 in the aggregate (mol/dm^2), respectively. The subscript or superscript "n" in Eq. 7 or 8 denote the aggregation number distinguishable from the spectra. Since the total concentration of MgPc(SEt)_8, C_T, is

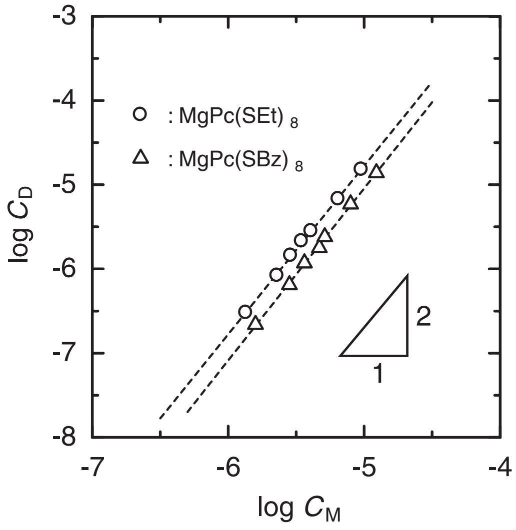

Fig. 2. Plots of $\log C_\text{D}$ vs $\log C_\text{M}$ for MgPc(SEt)_8 (open circle) and MgPc(SBz)_8 (open triangle) in toluene. The broken lines are the least-squares fitted ones, which slopes were close to 2. The correlation coefficient was larger than 0.99 for both plots.

$$C_\text{T} = [\text{MgPc(SEt)}_8]_\text{o} + \{[\text{MgPc(SEt)}_8]_\text{i} + n[(\text{MgPc(SEt)}_8)_n]\}\,\frac{S_\text{i}}{V_\text{o}}. \tag{9}$$

Equations 2, 8, and 9 can be combined to give,

$$\{[\text{MgPc(SEt)}_8]_\text{i} + n[(\text{MgPc(SEt)}_8)_n]_\text{i}\} = K_\text{agg}K'^n[\text{MgPc(SEt)}_8]_\text{o}^n + nK'[\text{MgPc(SEt)}_8]_\text{o}. \tag{10}$$

The stoichiometric analysis of the experimental data using Eq. 10 suggested the formation of the trimer ($n = 3$) of MgPc(SEt)_8 at the toluene/water interface. Interfacial adsorption and the aggregation parameter of MgPc(SEt)_8, K' (2.57×10^{-5} dm) and $K_{\text{agg}(n=3)}$ (2.93×10^{23} mol^{-2} dm^4), are shown in Table 2.

The stable crystal of the aqua complex, $\text{MgPc(H}_2\text{O)}$, has been reported, in which magnesium(II) ion is displaced by 0.496 Å from the plane of the Pc ring toward the coordinated oxygen of the water molecule.[35] Thus, it can be expected that the MgPc(SR)_8 derivatives adsorbed at the interface take the hydrated form of $\text{MgPc(SR)}_8\text{(H}_2\text{O)}$. The interfacial adsorptivity of MgPc(SR)_8 derivatives decreased in the order $\text{MgPc(SEt)}_8 > \text{MgPc(SBz)}_8 > \text{MgPc(SBh)}_8$. The decrease in the interfacial adsorption constant, K', by the replacement of the hydrogen atoms of the peripheral benzenes of MgPc with ethylthio-, benzylthio-, or benzhydrylthio-groups are thus ascribable to the enhanced lipophilicity or hydrophobicity. This was confirmed by the linear relationship between $\log K'$ and the molar volume of the substituents listed in Table 2 (Figure is not shown). Thus, the interfacial activity of MgPc(SR)_8 derivatives is afforded by the hydrated water and the hydrophobic groups.

2.4 Absorption Spectrum of Interfacial Aggregate of MgPc(SEt)_8. The adsorption spectrum of the aggregates of MgPc(SEt)_8 at the interface was directly measured by CLM

Table 2. Dimerization, Interfacial Adsorption, and Aggregation Constants of MgPc(SR)$_8$ Derivatives at 25 °C

	ε_M/dm^3 mol^{-1} cm^{-1} (λ_{max})$^{a)}$	ε_D/dm^3 mol^{-1} cm^{-1} (λ_{max})$^{b)}$	V_p/cm^3 mol^{-1} $^{c)}$	K_d/mol^{-1} dm^3 $^{d)}$	K'/dm$^{e)}$	$K_{agg(n=3)}$/mol^{-2} dm^4 $^{f)}$
MgPc(SEt)$_8$	1.10×10^5 (702 nm)	2.49×10^4 (655 nm)	75.5	1.54×10^5	2.57×10^{-5}	2.93×10^{23}
MgPc(SBz)$_8$	1.30×10^5 (708 nm)	3.69×10^4 (659 nm)	119.7	8.99×10^4	1.12×10^{-5}	—
MgPc(SBh)$_8$	2.51×10^5 (714 nm)	—	183.6	—	3.50×10^{-6}	—

a) ε_M; molar absorptivity of monomer, b) ε_D; molar absorptivity of dimer (expressed in terms of the monomer), c) V_p; estimated molar volume of one substituent, d) K_d; dimerization constant in toluene solution, e) K'; interfacial adsorption constant (= [MgPc(SR)$_8$]$_i$/[MgPc(SR)$_8$]$_o$), f) $K_{agg(n=3)}$; interfacial aggregation constant.

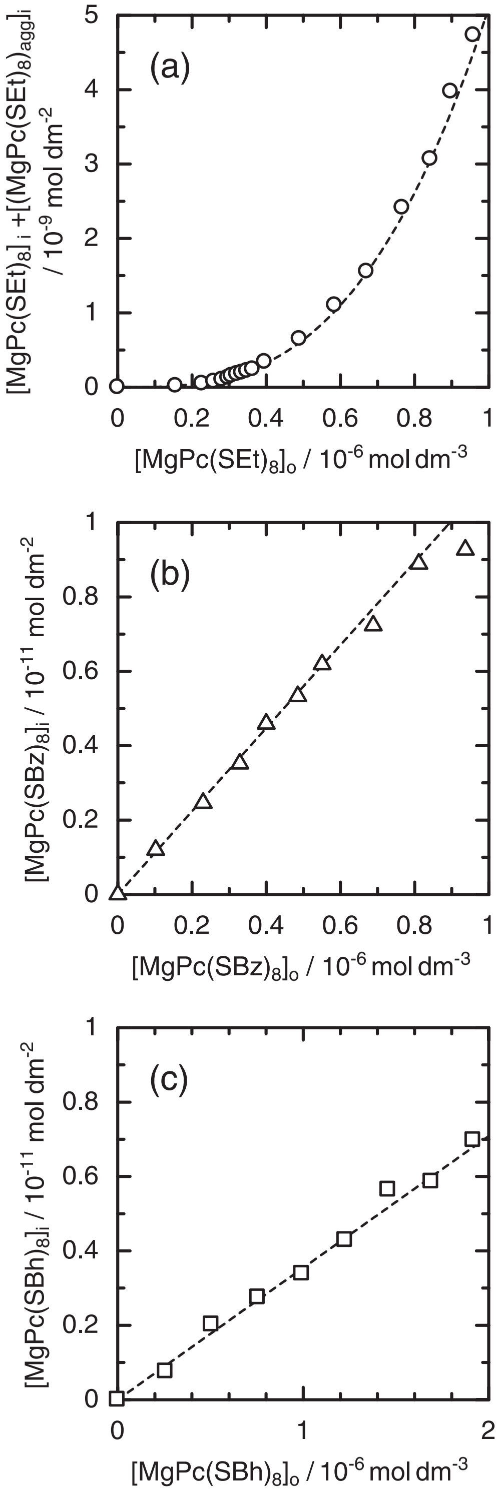

Fig. 3. The adsorption isotherms of (a) MgPc(SEt)$_8$, (b) MgPc(SBz)$_8$, and (c) MgPc(SBh)$_8$ measured by HSS method in the toluene/water interface at 25 °C. Each broken lines were obtained from the analysis with Eq. 1 or 10.

technique. Figure 4 shows the spectral changes due to the interfacial aggregation of MgPc(SEt)$_8$. Soon after the formation of the interface (up to 2 s), a new absorption peak appeared at the blue flank of the Q band. This peak is very similar to the dimer peak (655 nm) in a toluene solution of MgPc(SEt)$_8$.

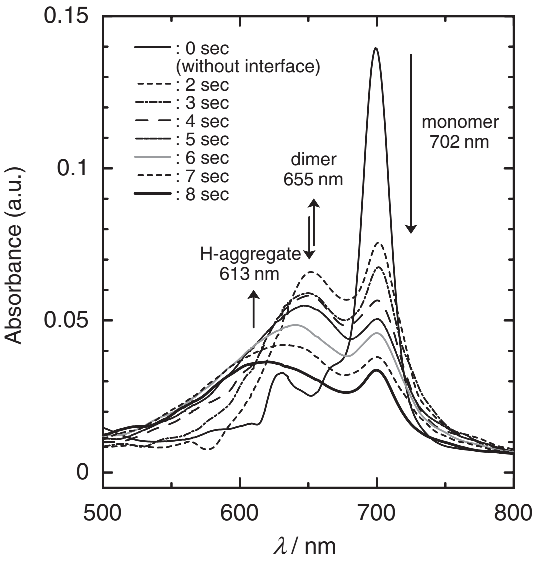

Fig. 4. The spectral change due to the interfacial aggregation of $MgPc(SEt)_8$ at the toluene/water interface measured by CLM technique. The absorption spectra were recorded at 1 s intervals until the adsorption equilibrium was achieved (8 s). The concentration of $MgPc(SEt)_8$ was 1.0×10^{-6} M. The arrows indicate the direction of the spectral changes with the time course.

Therefore, it can be concluded that the dimer was formed at the initial stage at the interface. The dimer band then decreased with the reaction time, and the blue-shift became more pronounced. The λ_{max} shifted from 702 to 613 nm after 8 s without an isosbestic point. The rise in the absorbance around 613 nm might be ascribed to another aggregate species (probably H-aggregate[36]). Higher aggregates of Pc usually show a new band in the same region as the dimer Q band, with broader and lower intensity.[37–40] Therefore, the present case may be a new one in Pc aggregation. In the case of $MgPc(SBz)_8$ and $MgPc(SBh)_8$, no spectral change was observed in the toluene/water system (Spectra are not shown).

Assuming that the interfacial spectra were composed of three Gaussian peaks of monomer, dimer and H-aggregate, the absorbance changes of the three individual peaks were obtained as a function of time. As for the spectra of the monomer, the most intense peak was used for this analysis. An example of such an analysis is shown in Fig. 5a. The deconvolution (minimization of χ^2 criterion) exhibited a good fit for all spectra, resulting in three distinct bands having the maxima (λ_{max1}, λ_{max2}, and λ_{max3}) at 702, 655, and 613 nm for monomer, dimer, and H-aggregate, respectively. This analysis revealed that the three bands have different time profiles (Fig. 5b). The plots in Fig. 5b of each absorbance change suggested the two-step, three-stage processes. The first rapid adsorption occurred in the time range of 0–2 s, and the second slow adsorption followed in up to 8 s. The integrated dimer band at 2 s gradually decreased to zero, followed by the increase of the H-aggregate band. The monomer band decreased up to 6 s, and then kept constant. As observed by the CLM experiments, the liquid–liquid interface had a strong influence on the aggregation state of $MgPc(SEt)_8$, which proceeded from monomer to H-aggregate depending on the total interfacial concentration.

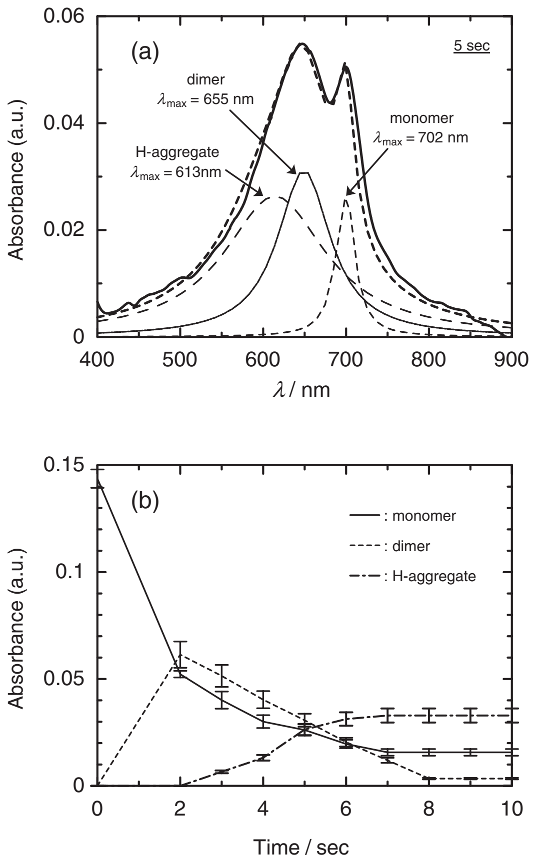

Fig. 5. (a) Example of deconvolution analysis; (b) time profile of the maximum absorbances of monomer, dimer, and H-aggregate.

2.5 The Extended Double-Dipole Model for $MgPc(SEt)_8$ H-Aggregate at the Interface.

Kohn et al.[41] proposed an extended dipole (ED) model to account for the blue- and red-shifts of the dye-aggregates. Moreover, Sakakibara et al. improved it to an extended double-dipole (EDD) model for the aggregation of phthalocyanine molecules.[42] The interaction integrals between Pc molecules in the aggregate are given by a series of various parameters, i.e., the number of aggregate molecules (*n*), the dipole length (*l*), the slipping distance (*d*), and the interplane distance (*h*). According to the EDD model, four charges ($\pm\mathcal{E}/2$ with distance *l*) are distributed at each corner of a square Pc molecule along *L*- and *M*-axis (see Fig. 6a, hereafter we call a moment along *L*-axis as *L*-component). The electrostatic interaction energy J_{12} between two paired dipoles is calculated by summarizing the *L*–*L* components and *M*–*M* components,

$$J_{12} = \frac{(\mathcal{E}/2)^2}{D}\left(\frac{1}{r_{11}} + \frac{1}{r_{12}} + \frac{1}{r_{21}} + \frac{1}{r_{22}} + \frac{1}{r_{33}} + \frac{1}{r_{34}} + \frac{1}{r_{43}} + \frac{1}{r_{44}} - \frac{1}{r_{13}} - \frac{1}{r_{14}} - \frac{1}{r_{23}} - \frac{1}{r_{24}} - \frac{1}{r_{31}} - \frac{1}{r_{32}} - \frac{1}{r_{41}} - \frac{1}{r_{42}}\right), \quad (11)$$

where *D* is the dielectric constant around the two dipoles ($D = 2.5$ the same value was used with Kohn et al.[41]), and r_{ab} (*a* or $b = 1$–4) is the distance between a point *a* on one molecule and a point *b* on another molecule (see Fig. 6b, c).

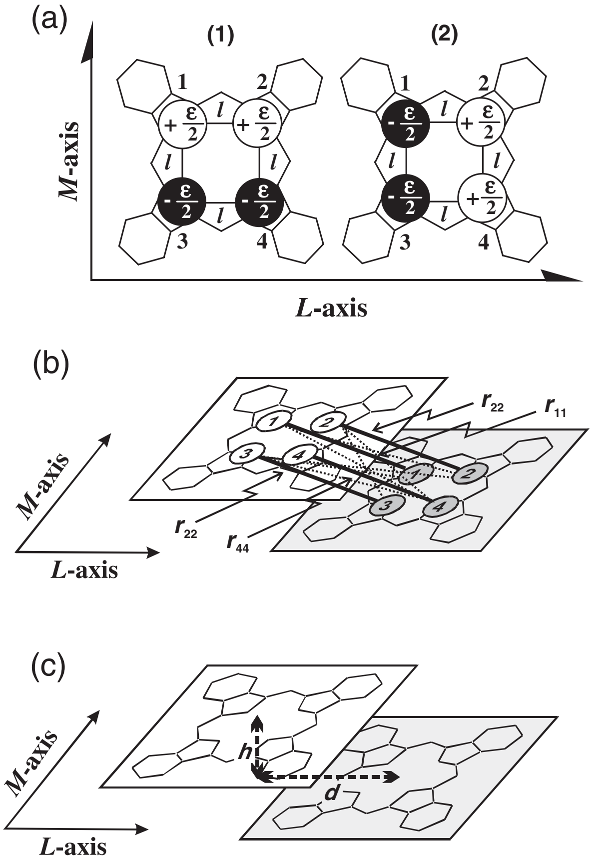

Fig. 6. (a) Extended double-dipole (EDD) model of Pc molecule of Sakakibara et al.[42] Each four charges ($\pm\mathcal{E}/2$) are located at the corners of Pc molecular plane separated by a distance l. The total moment exists along the M-axis in (1), and it exists along the L-axis in (2). (b) r_{ab} (a or $b = 1$–4) are distances between charges located on different molecules. (c) The interplane distance (h) and slipping distance (d) are sketched.

From this, the energy shift $\Delta E'$ of a dimer from a monomer equals $2J_{12}$.

The transition energy, ΔE_{agg}, of a Pc aggregate is then represented by the excitation energy of a Pc monomer ΔE_{m}, and the interaction integral $\Delta E'$, approximated by,

$$\Delta E_{\text{agg}} = \Delta E_{\text{m}} \pm \Delta E'. \tag{12}$$

In the case of the aggregate containing n molecules, the $\Delta E'$ value between the i-th and $(i+1)$-th Pc molecule with L–L components and M–M components is given as follows;

$$\begin{aligned}\Delta E' = \frac{2(\mathcal{E}/2)^2}{D}\sum^{n}\Bigg(&\frac{1}{R_{11}}+\frac{1}{R_{12}}+\frac{1}{R_{21}}+\frac{1}{R_{22}}\\ &+\frac{1}{R_{33}}+\frac{1}{R_{34}}+\frac{1}{R_{43}}+\frac{1}{R_{44}}-\frac{1}{R_{13}}-\frac{1}{R_{14}}\\ &-\frac{1}{R_{23}}-\frac{1}{R_{24}}-\frac{1}{R_{31}}-\frac{1}{R_{32}}-\frac{1}{R_{41}}-\frac{1}{R_{42}}\Bigg),\end{aligned} \tag{13}$$

where R_{ab} (a or $b = 1$–4) is the distance between a point a on the i-th molecule and a point b on the $(i+1)$-th molecule. The summation is performed over the whole aggregate.

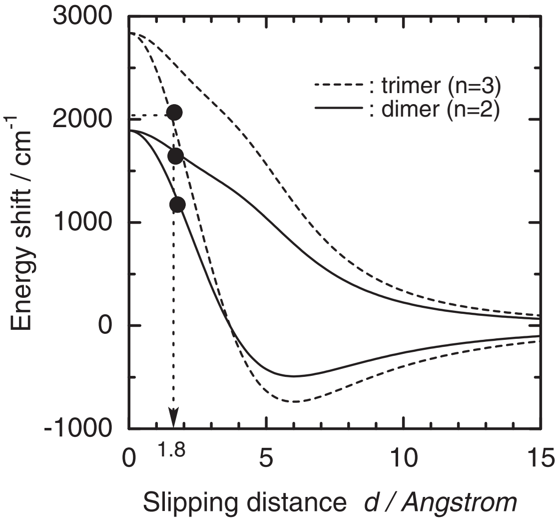

Fig. 7. The EDD model simulation of energy shift (cm^{-1}) of the two absorption bands shown as a function of slipping distance (Å). The interplane distance (h) and the dipole length (l) are fixed at 3.26 Å and 4 Å, respectively. The upper lines correspond to M–M components and the lower lines correspond to L–L components. n is the number of Pc moleculues.

The transition dipole moment μ ($= \mathcal{E}l$) is a constant given by the experimental data, for which we adopted 1.49 Debye for a MgPc monomer (this value was calculated from the oscillator strength (0.90) of the degenerate Q band[43]). The interplane distance (h) was set to 3.26 Å as reported for a MgPc crystal,[43] and this value was considered to be a typical van der Waals distance between Pc planes.[44–47] According to the procedure recommended by Sakakibara,[42] the dipole length (l) was fixed at 4 Å, and the slipping distance (d) was allowed to vary.

The calculated values $\Delta E'$ of L–L and M–M components for various arrangements are indicated in Fig. 7. In MgPc(SEt)$_8$ dimer at the toluene/water interface, the shift of the B band was 1615 cm^{-1} (blue-shift from 368 to 347 nm) and that of the Q band was 1022 cm^{-1} (blue-shift from 702 to 655 nm). Those values were fitted to the slipping distance of 1.8 Å (M–M components) and 1.9 Å (L–L components) with $n = 2$, respectively. In the case of a trimer ($n = 3$), which was observed in the HSS experiments, the calculated slipping distance corresponding to the blue-shift of 2068 cm^{-1} in the Q band (702 → 613 nm) of an H-aggregate was 1.8 Å (L–L components). These results suggest the existence of a dimer and trimer with a “face-to-face” arrangement between MgPc(SEt)$_8$ molecules.

Finally, the proposed mechanism for the interfacial adsorption and aggregation equlibria of MgPc(SR)$_8$ derivatives in the toluene/water system is summarized in Scheme 2. The observed parameters listed in Table 2 suggest that the MgPc(SR)$_8$ derivative, which tends to dimerize in the toluene solution, is more adsorbable into the interface and more easily forms the interfacial aggregate.

3. Conclusion

The interfacial adsorption and aggregation of MgPc(SR)$_8$ [R = Et, Bz, Bh] derivatives at the toluene/water interface

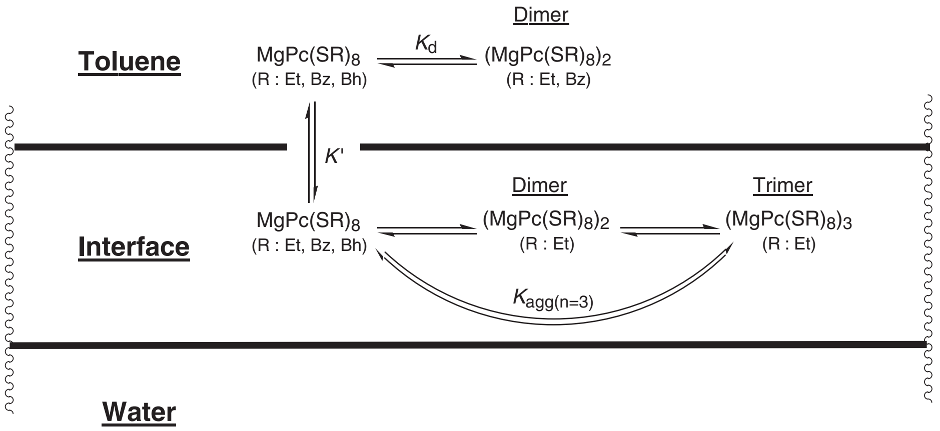

Scheme 2. Proposed scheme for the interfacial adsorption and aggregation mechanism of $MgPc(SR)_8$ derivatives in the toluene/water system.

was investigated by HSS and CLM methods. It was found that the interfacial adsorption behavior was affected by the hydrophobicity of the peripheral substituents. From the absorption spectra observed by CLM technique, it was found that the aggregation of $MgPc(SEt)_8$ at the toluene/water interface was a two-step, three-stage process, and that the final aggregate might be an eclipsed H-aggregate consisting of trimer units with a slipping distance of ca. 1.8 Å. The interfacial adsorption mechanism of Pc derivatives established in this study should be extended to novel phthalocyanine coordination chemistry, such as the interfacial catalytic synthesis with metal–phthalocyanine, and the design of self-assembled interfacial network-materials.

This study was supported by the Scientific Research of Priority Areas "Nano-Chemistry at the Liquid-Liquid Interfaces" (No. 13129204), the Grant-in-Aid for Scientific Research (S) (No. 16105002) of the Ministry of Education, Culture, Sports, Science and Technology and the Office of MORESCO under the contact education program. The authors thank Dr. Kenji Chayama of Konan University for his kind support in the synthesis of $MgPc(SR)_8$ derivatives. The author (K.A.) also thanks Dr. Naohiro Kanematsu of MORESCO (Kobe, Japan) for his helpful support in an early stage of this work.

References

1 "Phthalocyanines: Properties and Applications," ed by C. C. Leznoff and A. B. P. Lever, Vol. 1, VCH, New York, USA (1989); Vol. 2 (1992); Vol. 3 (1993).

2 I. Okura, "Photosensitization of Porphyrins and Phthalocyanines," Gordon and Breach Science Publishers, Netherlands (2000).

3 S. Palacin, *Adv. Colloid Interface Sci.*, **87**, 165 (2000).

4 C. M. Allen, W. M. Sharman, and J. E. Van Lier, *J. Porphyrins Phthalocyanines*, **5**, 161 (2001).

5 D. S. Terekhov, K. J. M. Nolan, C. R. McArthur, and C. C. Leznoff, *J. Org. Chem.*, **61**, 3034 (1996).

6 M. Hanack, A. Beck, and H. Lehmann, *Synthesis*, **1987**, 703; M. Hanck, A. Gül, A. Hirsch, B. K. Mandal, L. R. Subramanian, and E. Witke, *Mol. Cryst. Liq. Cryst.*, **1990**, 187.

7 J. H. Weber and D. H. Busch, *Inorg. Chem.*, **1965**, 469.

8 N. Kobayashi, H. Shirai, and N. Hojo, *J. Chem. Soc., Dalton Trans.*, **1984**, 2107.

9 M. Kandaz and Ö. Bekaroğlu, *Chem. Ber.*, **130**, 1833 (1997).

10 A. Gürek and Ö. Bekaroğlu, *J. Chem. Soc., Dalton. Trans.*, **1994**, 1419.

11 K. I. Ozoemena and T. Nyokong, *Inorg. Chem. Commun.*, **6**, 1192 (2003).

12 I. Benjamin, *J. Phys. Chem.*, **95**, 6675 (1991).

13 "Liquid Interfaces in Chemical, Biological, and Pharmaceutical Appreciations," ed by A. G. Volkov, Marcel Dekker, New York, USA (1997).

14 H. Watarai, K. Sasaki, K. Takahashi, and J. Murakami, *Talanta*, **42**, 1691 (1995).

15 H. Nagatani and H. Watarai, *Anal. Chem.*, **70**, 2860 (1998).

16 J. A. Riddick, W. B. Bunger, and T. K. Sakano, "Organic Solvents, 4th ed," John Wiley & Sons, New York, USA (1986).

17 M. E. Baguley, H. France, R. P. Linstead, and M. Whalley, *J. Chem. Soc.*, **1955**, 3521.

18 M. Whalley, *J. Chem. Soc.*, **1961**, 866.

19 H. Watarai, S. Tsukahara, H. Nagatani, and A. Ohashi, *Bull. Chem. Soc. Jpn.*, **76**, 1471 (2003).

20 H. Watarai, K. Takahashi, and J. Murakami, *Solvent Extr. Res. Dev., Jpn.*, **3**, 109 (1996).

21 H. Nagatani and H. Watarai, *Chem. Lett.*, **1997**, 167.

22 Y. Yulizar, A. Ohashi, and H. Watarai, *Anal. Chim. Acta*, **447**, 247 (2001).

23 H. Watarai and K. Satoh, *Langmuir*, **10**, 3913 (1994).

24 H. Watarai, M. Gotoh, and N. Gotoh, *Bull. Chem. Soc. Jpn.*, **70**, 957 (1997).

25 Y. Yulizar, A. Ohashi, H. Nagatani, and H. Watarai, *Anal. Chim. Acta*, **419**, 107 (2000).

26 D. Wöhrle, M. Eskes, K. Shigehara, and A. Yamada, *Synthesis*, **1993**, 194.

27 A. W. Snow and N. L. Jarvis, *J. Am. Chem. Soc.*, **106**, 4706 (1984).

28 D. D. Dominguez, A. W. Snow, J. S. Shirk, and R. G. S. Pong, *J. Porphyrins Phthalocyanines*, **5**, 582 (2001).

29 K. A. Conners, "Binding Constants," John Wiley & Sons, New York, USA (1987), pp. 141–187.

30 E. S. Dodsworth, A. B. P. Lever, P. Seymour, and C. C. Leznoff, *J. Phys. Chem.*, **89**, 5698 (1985).

31 H. J. Xu and G. X. Xiong, *J. Photochem. Photobiol., A*, **92**, 35 (1995).

32 H. Sigel, P. Waldmeierer, and B. Prijs, *Inorg. Nucl. Chem.*

Lett., **7**, 161 (1971).

33 N. Kobayashi, M. Togashi, T. Osa, K. Ishii, S. Yamauchi, and H. Hino, *J. Am. Chem. Soc.*, **118**, 1073 (1996).

34 S. Pearce and W. West, *J. Phys. Chem.*, **69**, 1894 (1965).

35 M. S. Fischer, D. H. Templeton, A. Zalkin, and M. Calvin, *J. Am. Chem. Soc.*, **93**, 2622 (1971).

36 W. West and B. H. Carroll, *J. Chem. Phys.*, **19**, 417 (1951).

37 N. Kobayashi and A. B. P. Lever, *J. Am. Chem. Soc.*, **109**, 7433 (1987).

38 W. A. Nevin, W. Liu, and A. B. P. Lever, *Can. J. Chem.*, **65**, 855 (1987).

39 Y. C. Yang, J. R. Ward, and R. P. Seiders, *Inorg. Chem.*, **24**, 1765 (1985).

40 A. Escosura, M. V. Martínez-Díaz, P. Thordarson, A. E. Rowan, R. J. M. Nolte, and T. Torres, *J. Am. Chem. Soc.*, **125**, 12300 (2003).

41 V. Czikkely, H. D. Föresterling, and H. Kohn, *Chem. Phys. Lett.*, **6**, 11 (1970).

42 Y. Sakakibara, K. Saito, and T. Tani, *Jpn. J. Appl. Phys.*, **37**, 695 (1998).

43 A. Endo, S. Matsumoto, and J. Mizuguchi, *J. Phys. Chem. A*, **103**, 8193 (1999).

44 J. Mizuguchi, *J. Phys. Chem. A*, **105**, 1121 (2001).

45 M. Brinkmann, P. Turek, and J. J. André, *J. Mater. Chem.*, **8**, 678 (1998).

46 C. J. Brown, *J. Chem. Soc. A*, **1968**, 2488.

47 R. F. Ziolo, C. H. Griffiths, and J. M. Troup, *J. Chem. Soc., Dalton. Trans.*, **1980**, 2301.